HAYATI
Journal of Biosciences

Vol. 32 No. 4, July 2025 840-849
DOI:10.4308/hjb.32.4.840-849
ISSN: 1978-3019
EISSN: 2086-4094

Research Article

Check for updates

OPEN ACCESS

Effect of Phosphate-based Glass Porous Microspheres (P30) Loaded with Extracellular Vesicle on Osteoblast Behaviour: *In Vitro* Study

Sigit Daru Cahayadi[1], Nur Aisyah Nuzulia[1], Arief Boediono[3], Ifty Ahmed[4], Retno Wahyu Nurhayati[5,6], Yessie Widya Sari[2*], Berry Juliandi[1]

[1]Department of Biology, Faculty of Mathematics and Natural Sciences, IPB University, Bogor 16680, Indonesia
[2]Department of Physics, Faculty of Mathematics and Natural Sciences, IPB University, Bogor 16680, Indonesia
[3]Department of Anatomy, Physiology and Pharmacology, School of Veterinary Medicine and Biomedical, IPB University, Bogor16680, Indonesia
[4]Advanced Materials Research Group, Faculty of Engineering, University of Nottingham, Nottingham, NG7 2RD, U.K.
[5]Department of Chemical Engineering, Faculty of Engineering, Universitas Indonesia, Depok 16424 Indonesia
[6]Stem Cell Tissue Engineering Research Cluster, Indonesian Medical Education and Research Institute IMERI, Faculty of Medicine, Universitas Indonesia, Jakarta 10430, Indonesia

ARTICLE INFO

Article history:
Received November 4, 2024
Received in revised form January 14, 2025
Accepted January 24, 2025

KEYWORDS:
bone regeneration,
bioactive potential,
osteogenesis,
tissue engineering

ABSTRACT

Bioactive materials, particularly phosphate-based glasses (PBG), hold great promise in bone repair due to their controllable degradation rates and bioactivity. This study evaluated PBG porous microspheres (P30) loaded with extracellular vesicles (EVs) for bone tissue engineering, focusing on osteogenesis, EV uptake, and cell invasion. P30 concentrations (5P30, 10P30, 50P30, 100P30, 500P30) were tested for their effects on calcification, EV uptake, and cell migration. Results showed that 100P30 exhibited optimal conditions for osteogenesis and EV delivery, with the highest calcification areas at both Day 7 and Day 14 and the most efficient EV internalization. Meanwhile, 500P30 demonstrated the highest cell migration, supporting pre-osteoblastic migration at this concentration. These findings indicate that 100P30 is ideal for mineralization and EV uptake, while 500P30 enhances cell invasion. This study highlights P30's versatility as a biomaterial for bone regeneration, with specific concentrations tailored to different regenerative goals. These results underscore the potential of P30 microspheres loaded with EVs as an effective strategy for promoting bone repair and regeneration.

1. Introduction

Bioactive materials have been extensively explored for biomedical applications, particularly bone repair and regeneration. These materials have been made from certain compositions of glass, glass-ceramic, and/or ceramic (Nirwana *et al.* 2022). Silicate-based Bioglass 45S5, is a well-known bioactive material and was first discovered in 1969 by Professor Larry Hench, which has a composition of 45% SiO_2, 24.5% Na_2O, 24.5% CaO, and 6% P_2O_5 (wt%) (Hench 2006). Later, Phosphate-based glasses (PBG) were developed, and their main advantage is that they offer biotherapeutic advantages due to their bioactivity, controllable degradation rates, and hence the rate of ions released. PBGs also offer significant benefits for orthopaedic applications as their main chemical constituents are calcium and phosphate ions, which makes them especially suitable for bone repair and regenerative medicine applications (Keating *et al.* 2005; Pneumaticos *et al.* 2010).

The bioactivity of PBG materials, such as P30 porous microspheres, is highly relevant in enhancing osteoblast behavior. Their ability to form hydroxyapatite (HA) on their surfaces is a key mechanism for promoting bone regeneration, as demonstrated by characterization studies using simulated body fluids (SBF) (Hench 2006). The capacity of PBG to initiate HA formation has been

* Corresponding Author
E-mail Address: yessie.sari@apps,ipb.ac.id

previously reported (Islam *et al.* 2017), supporting their application in bone tissue engineering. Moreover, specific PBG formulations have upregulated pro-osteogenic genes like BMP2 and BMP4 and increased collagen production, including COL2A1, COL10A1, and COL5A1 (Vallittu *et al.* 2020).

Recently, PBGs have been produced as microspheres and uniquely porous microspheres using a novel single-stage flame spheroidisation process. The porous morphology provides PBGs with the higher surface area, which can be exploited to increase cell adhesion and improve the kinetics of iwalon release (Milborne *et al.* 2022). Porous PBGs of various compositions have recently been developed and investigated for their ability to enhance stem cell adhesion (De Melo *et al.* 2021). Phosphate (P_2O_5) is used as a network glass former with CaO, MgO, and Na_2O added as network modifiers (Walter *et al.* 2001). P_2O_5 content below 40 mol% has been shown to produce sufficiently stable formulations suitable as implant materials. Further studies have shown that P30 (which contains 30% P_2O_5, 26% CaO, 24% MgO, and 20% Na_2O - in mol%) revealed the highest number of pyro- and orthophosphate species, which resulted in a more stable glass surface as well as enhanced cell adhesion. This formulation was an ideal candidate for applications requiring biomaterials with cell recruitment capabilities and supporting tissue growth (Keating *et al.* 2005; Milborne *et al.* 2022).

Biomaterials have developed significantly since stem cell discoveries and their combinations, which led to new enhanced combination developments, including Extracellular Vesicles (EV) (Swanson and Mishina 2022). EVs are small particles bound by lipid membranes secreted by most cell types and present in some biological fluids, such as blood and urine, where they play a key role in cell-to-cell communication. Based on their size, the EV population can be divided into exosomes (30-200 nm in diameter), microvesicles (200-1,000 nm in diameter), and apoptotic bodies (>1,000 nm in diameter) (Doyle and Wang 2019). The fact that EVs carry functional molecules which can modulate target cell responses opens the possibility of using EVs as next-generation biomaterials and is further supported by their low immunogenicity (Kou *et al.* 2022). Bone-relevant cell types have been shown to secrete EVs that regulate bone homeostasis, and recent evidence suggests that EV therapy is at least as efficient as cell therapy in eliciting bone regeneration in animal models of large bone defects (Yan *et al.* 2020; Infante *et al.* 2022). There are several advantages of using cell-derived factors, such as EVs, compared to stem cells alone. Cell-derived factors cannot self-replicate, indicating low tumorigenicity. Their high biocompatibility and low immunogenicity allow them to be distributed across the blood-brain barrier. In addition, their encapsulation ability can be loaded by specific drugs. Furthermore, they can be mass-produced by several culture generations and thawing, and they still maintain their effectiveness even after repeated freezing and thawing because of their lipid structure (Kou *et al.* 2022; Davies 2023).

Preliminary *in vivo* tests regarding the bioactive potential of PBG porous microspheres have been carried out (McLaren *et al.* 2019). In that study, *in vitro* tests were first performed using human bone marrow-derived mesenchymal stem cells (hBM-MSC) cell culture. The results indicated the presence of bioactivity in porous P40 glass microspheres, as shown in histological tissue assessment via H&E staining. New connective tissue stained in pale pink was built between biomaterials, acting as a support structure for bridging connective tissue growth between surrounding tissue and new tissue. Furthermore, hBM-MSC colonies were observed not only on the surface of the porous microspheres but also migrating into their pores (McLaren *et al.* 2019). Building on this, PBG porous microspheres (P30) were investigated *in vitro* to determine their efficacy for bone tissue engineering. The study involved loading concentrations of mice osteoblast cell-derived EVs into various P30 concentrations of 5 µg, 10 µg, 50 µg, 100 µg, and 500 µg to 0.1 ml EV. The EV-loaded P30 microspheres were then administered into osteoblast culture, and cell proliferation, cell homing, cell invasion, and calcification were analyzed to determine the optimal concentration of P30 for osteogenic processes.

2. Materials and Methods

2.1. Materials

This study was conducted following approval from the Animal Ethics Committee of the School of Veterinary Medicine and Biomedical Sciences, IPB University (Ethic Number: 190/KEH/SKE/III/2024). Porous P30 microspheres were manufactured utilizing the flame spheroidization technique (Milborne *et al.* 2022; Nuzulia *et al.* 2022). EVs (with a protein content of 8.76 µg/µL) were obtained from the IMERI Laboratory, Universitas Indonesia. The EVs were isolated from the secretome of the human umbilical cord, which were isolated from Mice Osteoblast Cell line MC3T3-E1 subclone-4 (ATCC CRL 2593). All chemicals were of analytical

grades: Dulbecco's modified eagle medium (DMEM) (Gibco, USA), Fetal Bovine Serum (Corning, USA), penicillin (Gibco, USA), streptomycin (Gibco, USA), beta glycerophosphate (Sigma, USA), 50 ng/ml ascorbic acid (Sigma, USA).

2.2. Methodologies

2.2.1. Mixing Extracellular Vesicle with P30

Prior to the *in vitro* study, P30 microspheres were sterilized by gamma irradiation without deforming their morphology. To evaluate the effect of EVs loading into P30 for the osteogenic process, varying amounts of P30 were soaked into 0.1 ml EVs and 1 ml standard cell culture medium (SC) consisting of Dulbecco's modified eagle medium (DMEM) supplemented with 10% Fetal Bovine Serum, 1% penicillin, and 1% streptomycin. We evaluated the following concentrations: 5, 10, 50, 100, or 500 µg P30 in 0.1 ml EV. These loading correlates with the sample codes used of 5P30, 10P30, 50P30, 100P30, and 500P30, respectively. As for comparison, we also evaluated the presence of P30 microspheres without EVs and labeled these as our control.

2.2.2. Osteogenesis

An *in vitro* osteogenesis assay was used to evaluate the calcification. The MC3T3-E1 mice osteoblast cells were cultivated in 12-well plates using SC media, with each well containing 10,000 cells. Subsequently, the cells underwent an incubation period lasting 18-20 hours at 37 °C, maintaining a 5% CO_2 concentration to facilitate their growth and development. Then, the SC media was replaced with Osteocyte differentiation media (SC media with added 10 mM beta glycerophosphate and 50 ng/ml ascorbic acid), and each P30 sample was introduced to the cells. The incubation period lasted until day 14 at 37°C and a 5% CO_2 concentration. A total of 12 chambers were prepared, corresponding to 5 samples with P30, 1 sample without P30, and 2 sampling times: day 7 and day 14.

After incubation, the supernatant containing cellular secretions was carefully harvested on day 7 and day 14. The harvested supernatant was then cold stored at a temperature of -80°C. Subsequently, alizarin red staining (1%, w/v, G1452; Solarbio, China) was employed to visualize and assess calcium deposition within the cellular structures and investigate the mineralization process and any calcium-related phenomena within the cultured cells. For this, the cell was stained with the alizarin red working solution and washed with distilled water.

Finally, microscopic observations (Inverted Microscope Nikkon, Diaphot, Japan) were conducted to analyze calcium deposits' cellular morphology and distribution. This comprehensive approach provided valuable insights into the cellular responses, differentiation, and mineralization processes under investigation. ImageJ settings used were RGB, Threshold, Inverse, and Measure. The calcification was evaluated by measuring the calcification area of the stained cells. The calcification area is calculated as the percentage ratio of the calcified area to all areas.

2.2.3. Extracellular Vesicle Uptake

Extracellular Vesicle Uptake is a measurement to assess how well EVs can penetrate cells to further affect their behavior. EV uptake assessment was conducted using a modified protocol from a previous study (Carpintero-Fernández *et al.* 2017). In the first step of this study, cells were cultivated in growth media using Chamber slide 8-well plates, with each well containing 5,000 cells. The cells were then left to incubate for a period of 18-20 hours at a temperature of 37°C, maintaining a 5% CO_2 concentration to support their growth and development. Samples with varied P30 EV concentrations were introduced to the culture using a micropipette. The culture was incubated over a 48-h incubation period at 37°C, with a 5% CO_2 concentration. Subsequently, the cells underwent a thorough rinsing with phosphate-buffered saline (PBS), and a 4',6-diamidino-2-phenylindole (DAPI) staining procedure was conducted. This staining method allowed for visualizing cell nuclei by imparting a distinctive color.

In the final step, cells were carefully examined under a microscope to assess their morphology and to observe any fluorescence staining. This comprehensive approach provided valuable insights into the cultured cells' cellular responses, structural characteristics, and nuclear features. All cells were counted manually.

2.2.4. Cell Invasion

Cell invasion assay measures cell mobility towards the target tissue. In this study, we used a transmigration insert assay with 8um pore size (BD Falcontm), following the previous study protocol (Stoellinger and Alexanian 2022). The first step was the preparation of 24-well plates, which contained SC media and attractant (Collagen (2% (w/v)). The initial cultured cells were placed in transmigration inserts and then placed on top of the well plates. Cells were cultured under 5% CO_2 and in a 37°C environment for 24 h. After that, the insert was

removed, and well plates were stained with 0.2% violet crystal. All samples were observed using a microscope to count the number of migrated cells. Microscopic observation was conducted using Inverted Microscope (Nikkon, Diaphot, Japan). All observation images were captured and analyzed using Image J Software (U. S. National Institutes of Health, Bethesda, Maryland, USA). Acquired data is then processed in IBM SPSS Statistics (Version 26).

ImageJ was used to measure the number of cells that had been migrated automatically. Settings that were used in this study were 8Bit, Invert LUT, Binary Mode, Binary Mask, Binary Watershed, Measure Particles.

2.2.5. Statistical Analysis

All data obtained by Image J processing were then analyzed by IBM SPSS Statistics version 26. The distribution of data was assessed using a Shapiro-Wilk analysis. Normally distributed data were expressed as Mean±SD, whilst abnormal distributions were expressed as Median (IQR). A comparison analysis of ANOVA and Kruskal Wallis was chosen based on this. Any significant results were further analysed into Post Hoc or Dunn's test analysis. A statistical significance was determined by the P value under 0.05 ($P<0.05$).

3. Results

3.1. Osteogenesis

The osteogenic property was initially assessed using the unstained culture, as shown in Figure 1. This culture revealed clear morphological changes, with osteoblasts transitioning into osteocytes, indicating early signs of osteogenesis. The observation of these morphological changes, such as the elongation and dendritic projections of osteocytes, confirmed that the differentiation process had begun. These findings validated the potential for further stained analysis. Therefore, subsequent analyses were performed on Day 7 (D7) and Day 14 (D14) to evaluate the progression of osteogenesis.

Microscopic images of alizarin red-stained cells with the addition of EVs at D7 and D14 further confirmed calcification. Calcified areas appeared as red-stained regions, while areas other than the red-stained or calcified regions were identified as uncalcified matrix (Figure 2). This distinction allowed for a quantifiable calcification assessment, demonstrating the osteogenic potential of P30 microspheres when combined with EVs.

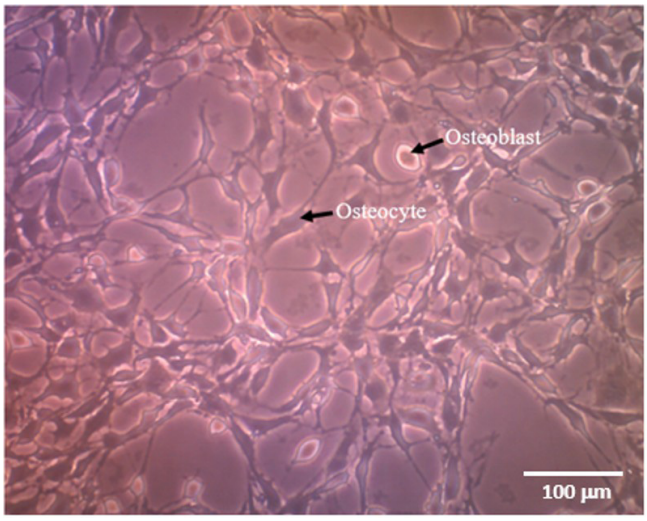

Figure 1. Microscopic image of unstained cells with 5P30 at Day 7, showing morphological transitions from osteoblasts to osteocytes

Image processing analysis was conducted using Fiji ImageJ to identify the percentage of calcified areas. Image processing detected color differences within the image, distinguishing darker regions (calcified) from brighter regions (uncalcified). The software calculated the percentage area of the darker regions. The data shows that the calcification area increased with the addition of P30, reaching a peak at 100P30 on Day 7 (D7). A similar peak was observed at 100P30 on Day 14 (D14) (Figure 3).

The D7 and D14 data were analyzed using an ANOVA test, which revealed a statistically significant difference across all groups at D7 ($P<0.01$) and D14 ($P<0.01$). A post hoc analysis indicated that 50P30 and 100P30 concentrations exhibited statistically significant differences from the control group ($P<0.01$) for both D7 and D14. However, further clarification may be needed to confirm whether the 50P30 concentration is equally significant at D14.

3.2. Extracellular Vesicle Uptake

Fluorescence staining was employed in this study to evaluate EV uptake by the targeted cells. Fluorescent agents such as PKH and DAPI were used to stain the EV membrane and viable cells. The results demonstrate the successful internalization of EVs by cells at different concentrations of P30 (Figure 4). Viable cells under the microscope appeared blue, while cells successfully internalized EVs exhibited green fluorescence. Figure 4 highlights that EV uptake increased with the P30 concentration,

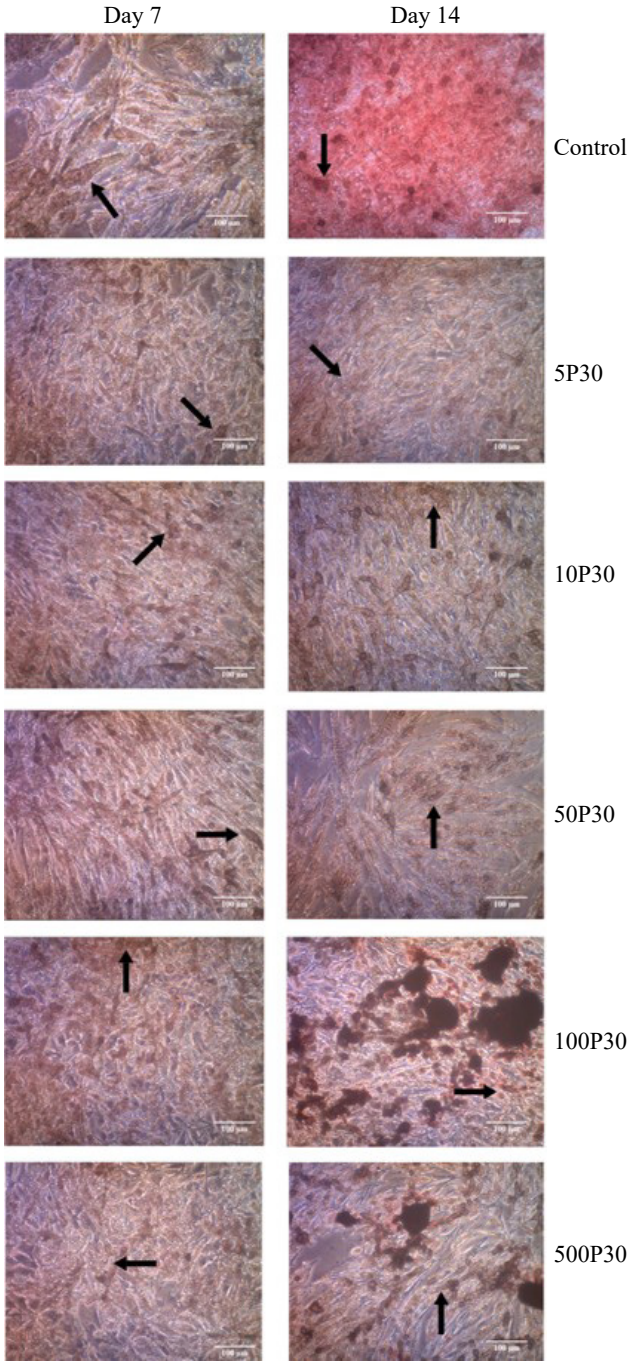

Figure 2. Microscopic images of stained cells using Alizarin Red at Day 7 (D7) and Day 14 (D14), with the addition of EVs across varying P30 concentrations

peaking at 100P30, indicating that 100P30 provides the most efficient sustained release and delivery of EVs, enhancing their internalization by the cells.

The efficiency of EV uptake was calculated as a percentage of cells with EVs compared to the total number of cells. The percentage of cells that successfully internalized EVs is shown in Figure 5, which highlights

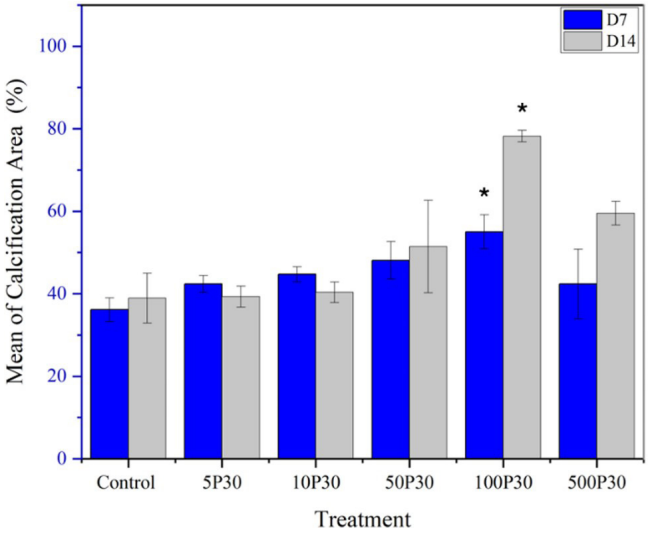

Figure 3. The mean percentage calcification area on Day 7 (D7) and Day 14 (D14) showed a peak at 100P30 concentration (n = 5). The asterisk (*) indicates statistically significant differences compared to other groups ($P<0.05$). The vertical lines on each bar represent the standard deviation

that EV uptake significantly increases with higher concentrations of P30, peaking at 100P30. ANOVA analysis revealed a significant difference among the groups ($P<0.01$). A post hoc test was conducted for each pair of groups with the control. The results demonstrated that 50P30 and 100P30 concentrations differed significantly from the control group ($P<0.01$). These findings indicate that both concentrations provide an optimal delivery of EVs, with 100P30 exhibiting the highest efficiency (Figure 5).

3.3. Invasion Assay

The invasion assay provides insights into how well cells respond to a stimulus or attractant. In this study, the highest number of invaded cells occurred at 500P30, indicating that this concentration promotes optimal cell invasion (Figure 6). The mean number of cells that migrated across an 8 µm pore size increased significantly with higher P30 concentrations, suggesting a dose-dependent response to P30 microspheres loaded with EVs.

The histological appearance of invaded cells depict purple-stained osteoblast or osteocyte nuclei, pink-stained matrix, and white pearly-stained P30 microspheres (Figure 7). At 500P30, the density of purple-stained nuclei was the highest, consistent with the quantitative data from Figure 6. Lower concentrations, such as 5P30 and 10P30, exhibited fewer invaded cells, while moderate concentrations,

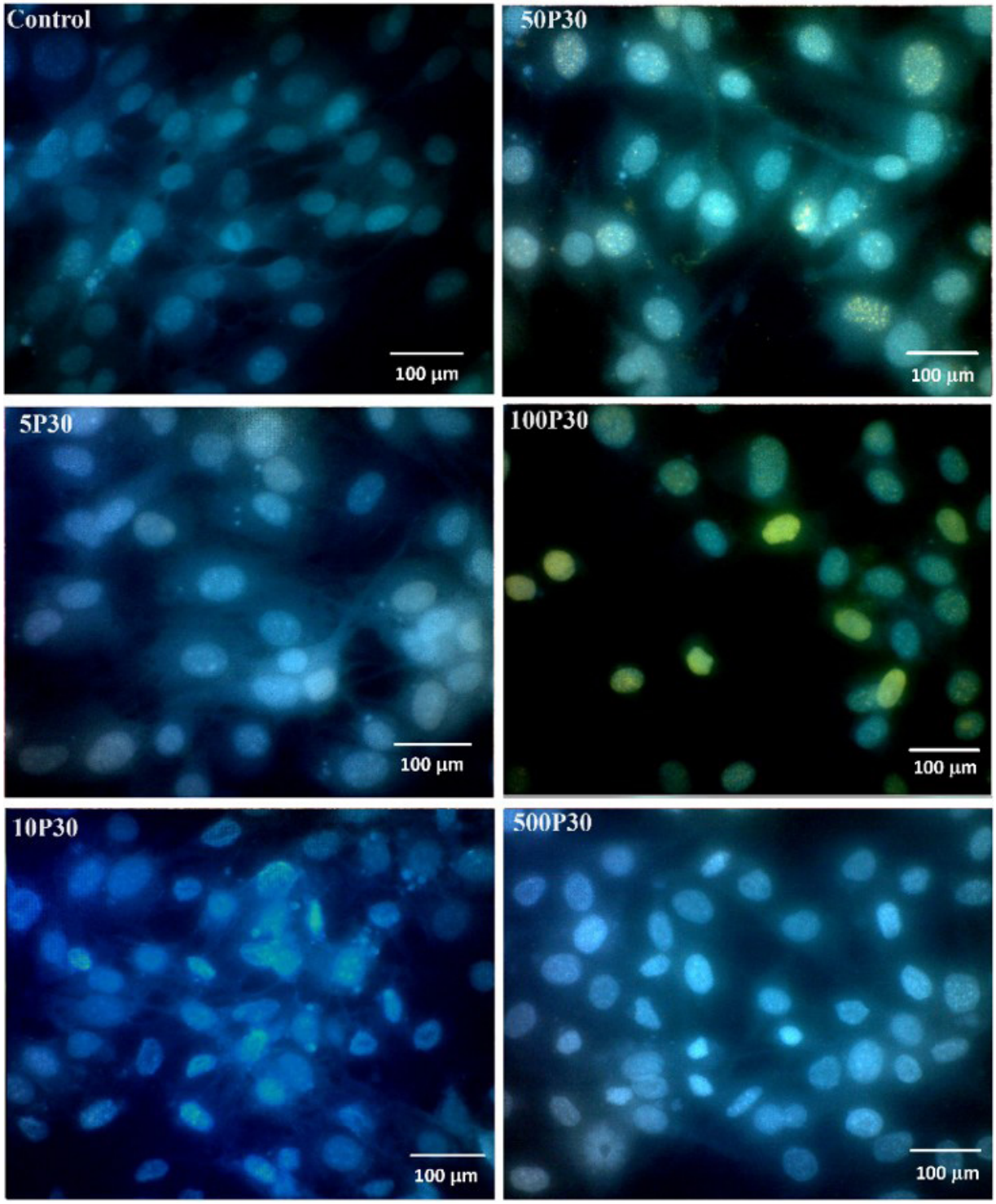

Figure 4. EV Uptake measurement using various P30 concentrations. The green stained nuclei indicate EVs presence in cells

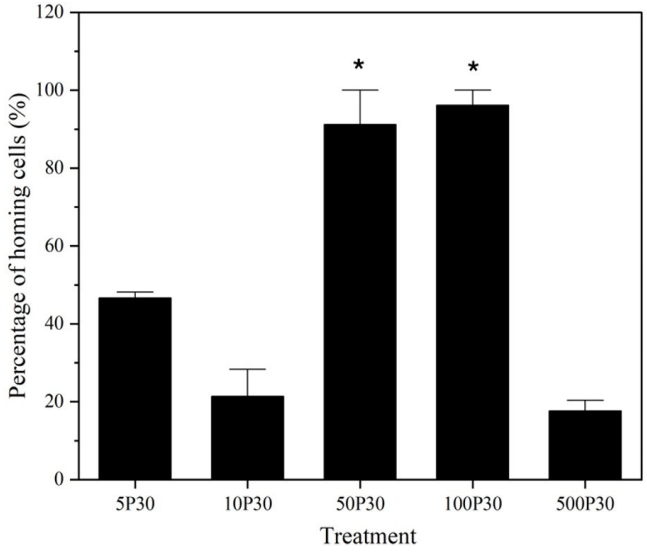

Figure 5. Percentage of cells successfully penetrated by extracellular vesicles (EVs) under different treatment conditions. The asterisk (*) indicates statistically significant differences compared to the 5P30 group (P<0.05). The vertical lines on each bar represent the standard deviation

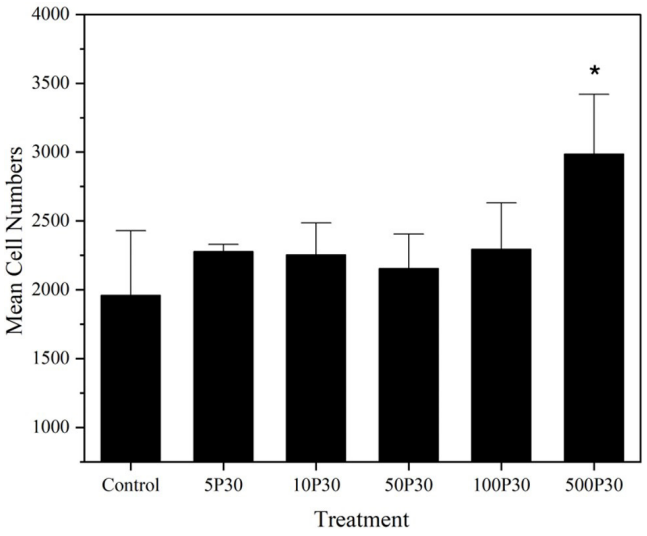

Figure 6. The mean number of cells migrated across an 8 µm pore size under different P30 treatments. The asterisk (*) indicates a statistically significant difference compared to the control group (P<0.05). The vertical lines on each bar represent the standard deviation

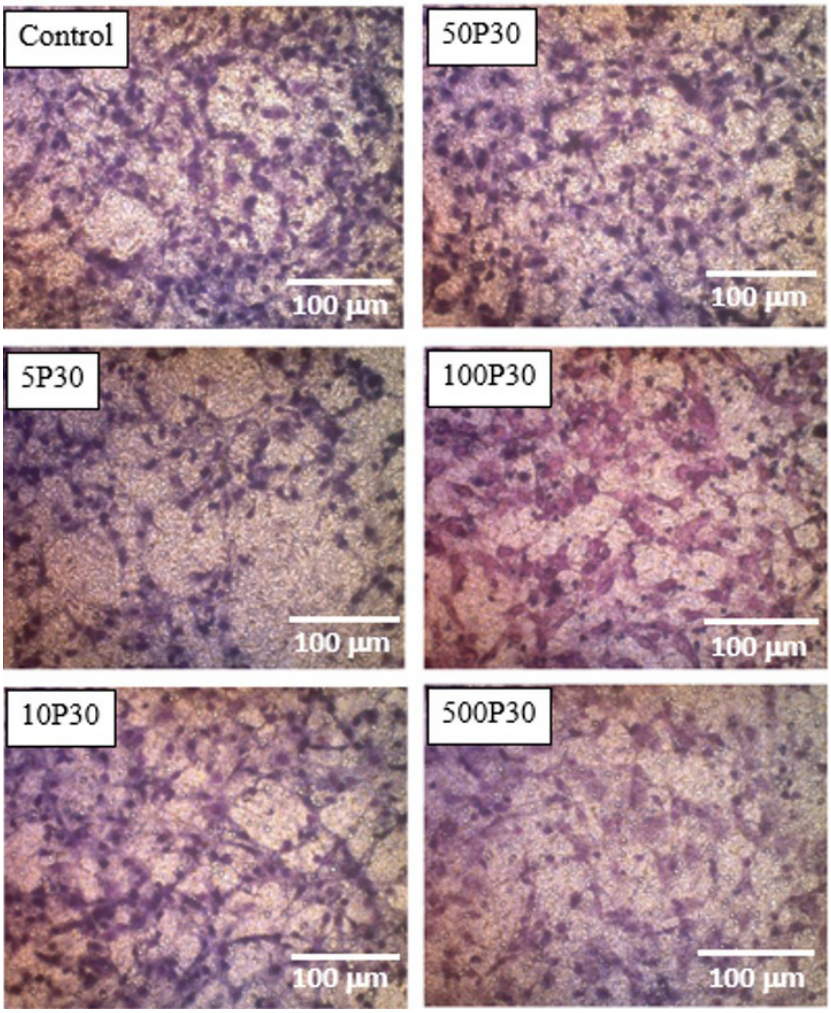

Figure 7. Microscopic images from the invasion assay show osteoblast or osteocyte nuclei (purple), matrix (pink), and P30 microspheres (white pearly-stained)

such as 50P30 and 100P30, showed an intermediate increase. These findings suggest that 500P30 provides the most effective environment for cell invasion, supporting its potential use in promoting cellular migration and osteogenesis.

Normality test results showed the data were evenly distributed ($P>0.05$). ANOVA test showed a significant cell numbers difference between all groups ($P<0.01$). The analysis then continued to Post Hoc analysis. The test found that migrating cell numbers at 500P30 significantly differed from those of other groups.

4. Discussion

4.1. Osteogenesis

The stained analysis showed a higher calcified area in the treatment groups, reflecting increased mineralization activity, which corresponds to the osteoconductive effect of treatments, as previously reported (Declercq *et al.* 2005). Detailed observations from earlier studies revealed that EVs help increase alkaline phosphatase (ALP) expression as early as Day 3 of treatment, initiating mineralization processes by Day 7 (Holkar *et al.* 2024). In this study, the mineralization process was influenced by the biological agent (EVs) and environmental factors such as P30 concentration.

The EV concentration of 8760 µg/ml used in this study was selected based on previous findings, which tested concentrations ranging from 0 µg/ml to 90 µg/ml. Higher EV concentrations, such as 90 µg/ml, have shown a significant increase in ALP expression compared to controls (1.47-fold; $P<0.01$). While this study hypothesizes that 100-fold higher EV concentrations could further enhance ALP expression and mineralization, further experiments are recommended to validate this. Nevertheless, the 100-fold EV concentration used here proved safe for osteoblasts, as no cellular debris was observed. Additionally, the type of EV plays a crucial role; matrix vesicles, a subtype rich in pre-calcified components like calcium and phosphorus, were found to accelerate secondary mineralization (Ansari *et al.* 2021).

Besides EVs, administered biomaterials like P30 are vital in promoting osteogenesis. The osteoconductive properties of P30 biomaterials were initially assessed by observing the deposition of hydroxyapatite (HA) layers on the surface. As noted by Islam *et al.* (2017), lower phosphate ion concentrations enhance the bioactivity of P30 by controlling ion release rates. This result emphasizes the importance of optimizing biomaterial composition. Furthermore, adding Na_2O or TiO_2 to P30 formulations has improved CaP nucleation and bioactivity (Islam *et al.* 2021). In this study, P30 promoted calcium and phosphate ion release upon degradation, facilitating mineralization.

The calcification area observed in this study varied with P30 concentration. The results showed that 100P30 achieved significantly higher calcification areas than the control group ($P<0.01$). This result suggests that 100P30 provides an optimal balance between mineralization and biomaterial degradation rates. Hypothetically, this concentration exhibits superior mineralization potential due to controlled ion release and optimal EV delivery. Further studies are needed to explore the long-term effects of P30 degradation on calcification and bone regeneration.

4.2. Extracellular Vesicle Uptake

For the EV uptake assay, cell changes were visualized using fluorescence staining. Fluorescent labeling of extracellular vesicles before loading them into the microspheres enabled tracking of their delivery and uptake by osteoblasts. Specific fluorescent markers, such as DAPI, were used to identify osteogenic differentiation (Zhang *et al.* 2015). Additionally, antibodies conjugated with fluorescent dyes targeting osteogenic markers such as osteocalcin, alkaline phosphatase (ALP), or collagen type I can provide insights into the differentiation of stem cells or osteoprogenitor cells into osteoblasts (Islam *et al.* 2017; Vallittu *et al.* 2020).

The results of the EV uptake assay showed that the number of cells successfully internalizing EVs increased significantly up to the 100P30 concentration. Several factors contribute to EV uptake, including EV cell source, EV storage, EV administration, and delivery strategy (Esmaeili *et al.* 2022). This study focused on the delivery strategy using P30 as a delivery agent. The delivery agent ensures the sustained release of EVs, facilitating better cellular internalization (Hu *et al.* 2022). The results indicated that 50P30 and 100P30 hypothetically provided better-sustained EV release than other concentrations.

The superior uptake observed at 100P30 may be attributed to the balance between the surface area of the porous microspheres and the optimal release of bioactive components, allowing efficient interaction with osteoblasts. Conversely, concentrations higher than 100P30, such as 500P30, showed reduced efficiency, potentially due to over-saturation of the delivery system or competition among EVs for cellular receptors. These findings suggest that while 50P30 and 100P30 are effective, further investigation into the mechanisms of EV release and cellular uptake at different concentrations is necessary to optimize the delivery system.

Future studies should explore the long-term effects of sustained EV release on osteogenic differentiation and bone regeneration. Additionally, the role of EV composition, particularly osteogenic growth factors such as BMP-2 or VEGF, could be examined to enhance understanding of how EVs mediate cellular responses when delivered using P30 microspheres.

4.3. Invasion Assay

The invasion assay in this study was designed to measure the ability of administered cells to migrate and penetrate surrounding host tissue. An indirect transwell migration assay was employed to minimize confounding factors. Osteoblasts cultured with EV+P30 in the top chamber were expected to migrate into the bottom chamber, filled with collagen as an attractant. EVs contain microRNAs, such as miR-424, that upregulate key osteogenic markers like osteocalcin (OCN), BMP2, and DMP-1 protein expression (Huang *et al.* 2023). This increased protein expression promotes osteoblast differentiation (Duggal *et al.* 2023).

Osteocytes expressing DMP-1 were attracted to the collagen matrix in the bottom chamber, as they tend to migrate toward lacunae, mimicking their natural microenvironment (Shiflett *et al.* 2019). Additionally, studies have shown that migrated osteocytes express higher levels of OCN, DMP-1, and SOST proteins, reinforcing their osteogenic activity (Uchihashi *et al.* 2013). This study quantified and compared the number of cells migrated into the bottom chamber across treatment groups.

The results revealed that 500P30 exhibited the highest number of invaded cells. This result suggests that P30 provided an optimal environment for osteoblast migration at this concentration, possibly due to its ability to enhance the sustained release of calcium and phosphate ions, which is critical for pre-osteoblastic activity. Another study supports this finding, showing that glass-based biomaterials like P30 possess superior calcium-dissolving abilities, promoting pre-osteoblastic migration (Kajander *et al.* 2023). Hypothetically, the combination of EVs and P30 at 500P30 creates a synergistic effect, providing bioactive signals and a conducive microenvironment that enhances cellular invasion.

However, while 500P30 showed the highest invasion, it is important to investigate further the potential limitations of this concentration, such as the saturation of bioactive signals or possible cytotoxic effects due to prolonged exposure to high ion concentrations. Future studies should explore the long-term impact 500P30 on osteoblast differentiation and functionality to confirm its optimal role in bone regeneration strategies.

In conclusion, this study demonstrates the potential of PBG porous microspheres (P30) loaded with extracellular vesicles (EVs) for bone regeneration. The findings highlight 100P30 as optimal for osteogenesis and EV uptake, with superior calcification and EV internalization, while 500P30 excels in promoting cell invasion facilitating pre-osteoblastic migration. The results underscore the need to tailor P30 concentrations for specific regenerative objectives. Future research should evaluate these biomaterials' long-term effects and *in vivo* efficacy in bone repair applications.

Acknowledgements

This study was funded by the Education Endowment Fund (LPDP) through the Research and Innovation for Advanced Indonesia (RIIM) program, the National Research and Innovation Agency (BRIN) with contract number (4/IV/KS/05/2023 & 13955/IT3/PT.01.03/P/B/2023). We would like to thank Dr. Silmi Mariya (LPPM-IPB Primate Animal Study Center) and Angga Saputra, M.Si. (Department of Physics, IPB University) for their technical assistance.

References

Ansari, S., de Wildt, B.W.M., Vis, M.A.M., de Korte, C.E., Ito, K., Hofmann, S., Yuana, Y., 2021. Matrix vesicles: role in bone mineralization and potential use as therapeutics. *Pharmaceuticals*. 14, 289. DOI: 10.3390/ph14040289

Carpintero-Fernández, P., Fafián-Labora, J., O'Loghlen, A., 2017. Technical advances to study extracellular vesicles. *Frontiers in Molecular Biosciences*. 4, 79. DOI:10.3389/fmolb.2017.00079

Davies, O.G., 2023. Extracellular vesicles: from bone development to regenerative orthopedics. *Mol. Ther.* 31, 1251-1274. DOI:10.1016/j.ymthe.2023.02.021

De Melo, N., Murrell, L., Islam, M.T., Titman, J.J., Macri-Pellizzeri, L., Ahmed, I., Sottile, V., 2021. Tailoring pyro- and orthophosphate species to enhance stem cell adhesion to phosphate glasses. *International Journal of Molecular Sciences*. 22, 837. DOI:10.3390/ijms22020837

Declercq, H.A., Verbeeck, R.M.H., De-Ridder, L.I.F.J.M., Schacht, E.H., Cornelissen, M.J., 2005. Calcification as an indicator of osteoinductive capacity of biomaterials in osteoblastic cell cultures. *Biomaterials.* 26, 4964–4974. DOI:10.1016/j.biomaterials.2005.01.025

Doyle, L.M., Wang, M.Z., 2019. Overview of extracellular vesicles, their origin, composition, purpose, and methods for exosome isolation and analysis. *Cells.* 8, 727. DOI:10.3390/cells8070727

Duggal, M.S., Lim, S.K., Toh, W.S., 2023. Mesenchymal stromal cell exosomes enhance dental pulp cell functions and promote pulp-dentin regeneration. *Biomater Biosyst.* 11, 100078. DOI:10.1016/j.bbiosy.2023.100078

Esmaeili, A., Alini, M., Eslaminejad, M.B., Hosseini, S., 2022. Engineering strategies for customizing extracellular vesicle uptake in a therapeutic context. *Stem Cell Res. Ther.* 13, 129. DOI:10.1186/s13287-022-02806-2

Hench, L.L., 2006. The story of Bioglass®. *Journal of Materials Science: Materials in Medicine.* 17, 967–978. DOI:10.1007/s10856-006-0432-z

Holkar, K., Kale, V., Pethe, P., Ingavle, G., 2024. The symbiotic effect of osteoinductive extracellular vesicles and mineralized microenvironment on osteogenesis. *J. Biomed. Mater. Res. A.* 112, 155–166. DOI:10.1002/jbm.a.37600

Hu, H., Zhang, H., Bu, Z., Liu, Z., Lv, F., Pan, M., Huang, X., Cheng, L., 2022. Small extracellular vesicles released from bioglass/hydrogel scaffold promote vascularized bone regeneration by transferring miR-23a-3p. *Int. J. Nanomedicine.* 17, 6201–6220. DOI:10.2147/IJN.S389471

Huang, C.C., Kang, M., Leung, K., Lu, Y., Shirazi, S., Gajendrareddy, P., Ravindran, S., 2023. Micro RNA based MSC EV engineering: targeting the BMP2 cascade for bone repair. *Front. Cell Dev. Biol.* 11, 1127594. DOI:10.3389/fcell.2023.1127594

Infante, A., Alcorta-Sevillano, N., Macías, I., Rodríguez, C.I., 2022. Educating EVs to improve bone regeneration: getting closer to the clinic. *Int. J. Mol. Sci.* 23, 1865. DOI:10.3390/ijms23031865

Islam, M.T., Felfel, R.M., Abou Neel, E.A., Grant, D.M., Ahmed, I., Hossain, K.M.Z., 2017. Bioactive calcium phosphate–based glasses and ceramics and their biomedical applications: a review. *J. Tissue. Eng.* 8, 204173141771917. DOI:10.1177/2041731417719170

Islam, M.T., Macri-Pellizzeri, L., Hossain, K.M.Z., Sottile, V., Ahmed, I., 2021. Effect of varying the Mg with Ca content in highly porous phosphate-based glass microspheres. *Materials Science and Engineering: C.* 120, 111668. DOI:10.1016/j.msec.2020.111668

Kajander, K., Sirkiä, S.V., Vallittu, P.K., Heino, T.J., Määttä, J.A., 2023. Bioactive glasses promote rapid pre-osteoblastic cell migration in contrast to hydroxyapatite, while carbonated apatite shows migration inhibiting properties. *Sci Rep.* 13, 20587. DOI:10.1038/s41598-023-47883-2

Keating, J.F., Simpson, A.H.R.W., Robinson, C.M., 2005. The management of fractures with bone loss. *The Journal of Bone and Joint Surgery.* 87-B, 142–150. DOI:10.1302/0301-620x.87b2.15874

Kou, M., Huang, L., Yang, J., Chiang, Z., Chen, S., Liu, J., Guo, L., Zhang, X., Zhou, X., Xu, X., Yan, X., Wang, Y., Zhang, J., Xu, A., Tse, H., Lian, Q., 2022. Mesenchymal stem cell-derived extracellular vesicles for immunomodulation and regeneration: a next generation therapeutic tool?. *Cell Death and Disease*. 13, 590. DOI:10.1038/s41419-022-05034-x

McLaren, J.S., Macri-Pellizzeri, L., Hossain, K.M.Z., Patel, U., Grant, D.M., Scammell, B.E., Ahmed, I., Sottile, V., 2019. Porous phosphate-based glass microspheres show biocompatibility, tissue infiltration, and osteogenic onset in an ovine bone defect model. *ACS Appl. Mater. Interfaces.* 11, 15436–46. DOI:10.5435/00124635-200501000-00010

Milborne, B., Murrell, L., Cardillo-Zallo, I., Titman, J., Briggs, L., Scotchford, C., Thompson, A., Layfield, R., Ahmed, I., 2022. Developing porous ortho- and pyrophosphate-containing glass microspheres; structural and cytocompatibility characterisation. *Bioengineering.* 9, 611. DOI:10.3390/bioengineering9110611

Nirwana, I., Munadziroh, E., Yuliati, A., Fadhila, A.I., Nurliana, Wardhana A.S., Shariff, K.A., Surboyo M.D.C., 2022. Ellagic acid and hydroxyapatite promote angiogenesis marker in bone defect. *J. Oral. Biol. Craniofac. Res.* 12, 116–20. DOI:10.1016/j.jobcr.2021.11.008

Nuzulia, N.A., Islam, M.T., Saputra, A., Sudiro, T., Timuda, G.E., Mart, T., Sari, Y.W., Ahmed, I., 2022. Developing highly porous glass microspheres via a single-stage flame spheroidisation process. *Journal of Physics: Conference Series.* 2243, 012005. DOI:10.1088/1742-6596/2243/1/012005

Pneumaticos, S.G., Triantafyllopoulos, G.K., Basdra, E.K., Papavassiliou, A.G., 2010. Segmental bone defects: from cellular and molecular pathways to the development of novel biological treatments. *J. Cell. Mol. Med.* 14, 2561–2569. DOI:10.1111/j.1582-4934.2010.01062.x.

Uchihashi, K., Aoki, S., Matsunobu, A., Toda, S., 2013. Osteoblast migration into type I collagen gel and differentiation to osteocyte-like cells within a self-produced mineralized matrix: a novel system for analyzing differentiation from osteoblast to osteocyte. *Bone.* 52, 102–110. DOI:10.1016/j.bone.2012.09.001

Shiflett, L.A., Tiede-Lewis, L.M., Xie, Y., Lu, Y., Ray, E.C., Dallas, S.L., 2019. Collagen dynamics during the process of osteocyte embedding and mineralization. *Frontiers in Cell and Developmental Biology.* 7, 1-16. DOI:10.3389/fcell.2019.00178

Stoellinger, H.M., Alexanian, A.R., 2022. Modifications to the transwell migration/invasion assay method that eases assay performance and improves the accuracy. *Assay Drug Dev Technol.* 20, 75–82. DOI:10.1089/adt.2021

Swanson, W.B., Mishina, Y., 2022. New paradigms in regenerative engineering: Emerging role of extracellular vesicles paired with instructive biomaterials. *Biocell.* 46, 1445-1451. DOI:10.32604/biocell.2022.018781

Vallittu, P.K., Posti, J.P., Piitulainen, J.M., Serlo, W., Määttä, J.A., Heino, T.J., Pagliari, S., Syrjänen S.M., Forte, G., 2020. Biomaterial and implant induced ossification: *in vitro* and *in vivo* findings. *J. Tissue. Eng. Regen. Med.* 14, 1157–68. DOI:10.1002/term.3056

Walter, G., Vogel, J., Hoppe, U., Hartmann, P., 2001. The structure of $CaO–Na_2O–MgO–P_2O_5$ invert glass. *Journal of Non-Crystalline Solids.* 296, 212–223. DOI:10.1016/s0022-3093(01)00912-7

Yan, H.C., Yu, T.T., Li, J., Qiao, Y.Q., Wang, L.C., Zhang, T., Li, Q., Zhou, Y., Liu, D.W., 2020. The delivery of extracellular vesicles loaded in biomaterial scaffolds for bone regeneration. *Frontiers in Bioengineering and Biotechnology.* 8, 1015. DOI:10.3389/fbioe.2020.01015

Zhang, L.X., Shen, L.L., Ge, S.H., Wang, L.M., Yu, X.J., Xu, Q.C., Yang, P.S., Yang, C.Z., 2015. Systemic BMSC homing in the regeneration of pulp-like tissue and the enhancing effect of stromal cell-derived factor-1 on BMSC homing. *Int. J. Clin. Exp. Pathol.* 8, 10261–10271.